

## Friction and Wear of Cr-O-N Coatings Characterized by Atomic Force Microscopy

T. Kuznetsova<sup>a</sup>, V. Lapitskaya<sup>a</sup>, S. Chizhik<sup>a</sup>, A.S. Kuprin<sup>b</sup>, G.N. Tolmachova<sup>b</sup>, V.D. Ovcharenko<sup>b</sup>, A. Gilewicz<sup>c</sup>, O. Lupicka<sup>c</sup>, B.Warcholinski<sup>c</sup>

<sup>a</sup> A. V. Luikov Heat and Mass Transfer Institute of the National Academy of Sciences of Belarus, Minsk, Belarus,

<sup>b</sup> National Science Center Kharkov Institute of Physics and Technology, Kharkov, Ukraine,

<sup>c</sup> Koszalin University of Technology, Faculty of Technology and Education, Koszalin, Poland.

### Keywords:

CrON  
AFM  
Friction  
Wear

### Corresponding author:

Bogdan Warcholinski  
Faculty of Technology and Education  
Koszalin University of Technology  
Koszalin, Poland.  
e-mail: [bogdan.warcholinski@tu.koszalin.pl](mailto:bogdan.warcholinski@tu.koszalin.pl)

### ABSTRACT

Cr-O-N coatings with different oxygen concentration were deposited using vacuum arc plasma fluxes on steel substrates. The coatings were investigated using atomic force microscopy under ambient temperature and humidity controlled conditions. The surface structure, friction and wear were investigated. The results indicate that coefficient of friction and friction force of Cr-O(50)-N coating consisted of Cr<sub>2</sub>O<sub>3</sub> phase tested in a sliding regime are the lowest compared to other Cr-O-N coatings characterized by cubic CrN phase. In the ploughing regime the Cr-O(20)-N coating is characterized by the lowest coefficient of friction of and the wear rate.

© 2019 Published by Faculty of Engineering

## 1. INTRODUCTION

The investigations of the Cr-N coatings used as protective coatings on tools (also resistant to corrosion), and machine parts have been carried out for many years. CrN coatings are widely applied in industry but their properties especially at higher temperature, are not always sufficient. The thermal stability of CrN coating limited to about 600°C can be improved (increased) by changing the chemical composition of the coating by addition of the third element. Oxygen as an additional element can improve selected mechanical properties, as hardness and elastic modulus [1]. Cr-O-N coatings have also better corrosion resistance than CrN and Cr<sub>2</sub>O<sub>3</sub> [2], better adhesion and a uniform structure [3].

Cr-O-N coatings can be applied both as a protective coating against oxidation and wear, but as well as the photo-thermal conversion of solar energy as a solar selective coating of the absorber [4], or as a decorative coatings due to their different color dependent on coating thickness and chemical and phase composition [5].

In Cr-O-N coatings two major structures appear: for low oxygen concentration CrN phase forms and for higher (above 43 at. %) Cr<sub>2</sub>O<sub>3</sub> phase forms [6]. Castaldi et al. suggested the synthesis of substitutional CrO<sub>x</sub>N<sub>1-x</sub> solid solution [1]. The hardness and elastic modulus of CrN phase increase with oxygen concentration in the coating and decrease for Cr<sub>2</sub>O<sub>3</sub> phase. It should be mentioned that the main topic of interest of

Cr-O-N coatings was the structure and morphology of coatings. The mechanical and tribological properties were not a major subject of investigations and were presented occasionally. Urgen et al. [7] found that the concentration of oxygen in the Cr-O-N coatings formed using reactive cathodic arc evaporation played a critical role on the tribological behavior. They observed the temperature independent wear behavior in the coatings produced with oxygen content higher than 46% and the coefficient of friction ranging from 0.2 to 0.5 dependent on chemical composition of the coatings and test temperature. The reciprocating testing system with load of 2 N, amplitude of 1 mm and 10 Hz frequency was used. The investigations using ball-on-disc system with normal load of 20 N and sliding speed of 0.2 m/s also indicate that coefficient of friction ranged from 0.45 to 0.65 dependents on oxygen concentration in CrN structure. The wear rate decreases with oxygen concentration and ranges from  $4.4 \times 10^{-6}$  to  $6.7 \times 10^{-8}$  mm<sup>3</sup>/Nm [8].

Cr-O-N coatings can be formed by many methods: cathodic arc evaporation [9], arc ion plating [10], pulsed laser deposition, magnetron sputtering [11].

Different values of coefficient of friction for CrN (tested in macro-scale), ranged from 0.4 to 0.87 and depend on many factors, among these: coating formation, test conditions - the nature of the counterbody, load, sliding speed, etc. are presented in literature. Ehasarian et al. [12] found that sputtered CrN tested in pin-on-disc device equipped with a 6 mm diameter Al<sub>2</sub>O<sub>3</sub> ball as a counterpart and a normal load of 5 N and linear speed of 0.1 m/s has coefficient of friction amounted to 0.45. Similar values were presented by Essen et al. [13]. A little lower coefficient of friction (0.37) was observed by Drnovsek et al. [14] in the same testing conditions. CrN coating deposited using cathodic arc evaporation under normal load of 20 N and sliding speed 0.2 m/s has coefficient of friction  $0.55 \pm 0.03$  [15]. The higher value is presented by Shi et al. [16]. CrN coating of about 20 μm in thickness deposited using arc ion plating and tested in ball-on-disc system equipped in cemented carbide ball (3 mm in diameter) under normal load of 10 N and sliding speed of 0.02 m/s has coefficient of friction of about 0.65. It should be mentioned that friction wasn't

previously tested in Cr-O-N coatings. It is known, however, that the increase in oxygen concentration in the coating increases the hardness [9]. It can therefore be supposed that such coatings will be characterized by a lower coefficient of friction.

The good tribological properties of thin coatings are determined by their surface properties. But the standard testing methods often destruct thin coating because of deflection of steel substrates, cracking of coating and scratching the coating by debris particles [13]. So the real tribological surface properties of the coatings remain without testing. Atomic force microscopy (AFM) is the most suitable multifunctional technique with a high resolution both for topography and for force loading [17] to study the various surface phenomena of thin coatings, like morphology, roughness [18], adhesion, friction [19] and wear of the surface. Small normal forces (from several nanoNewtons till milliNewtons) applied during test, due to small contact area, can provide considerable Hertzian contact pressure in surface layers. After AFM wear test the results can be also visualized by AFM.

The friction and wear in microscale are different from the macroscale [17]. So the experimental investigations to determine the tribological properties of the Cr-O-N coating surface using AFM are very important due to its possible application in microcontacts and micromechanisms.

Some preliminary data on tribological properties including the AFM method are presented in [8]. It was found that the coefficient of friction of the coating with respect to diamond probe with radius of 200 nm and applied load 0.5 mN ranges from 0.1 to 0.3 dependent on its chemical composition. The wear rate depends on wear test conditions and ranges from  $1 \times 10^{-13}$  to  $2 \times 10^{-14}$  m<sup>3</sup>/Nm. It means that they are about two orders higher than the wear rate determined in ball-on-disc method [20].

There are many papers on Cr-O-N forming and characterization including structure [4], mechanical properties [10], tribological properties [7] in macro-scale. To the best of our knowledge they were not systematically tested in microscale. The aim of the work was to assess of tribological characteristics of Cr-O-N coatings (roughness, friction force and friction coefficient,

wear rate) in microscale, i.e. under conditions in which the coating is not damaged by cracks due to deformation of the substrate, as in the macroscale test.

## 2. EXPERIMENTAL DETAILS

### 2.1 Coatings deposition

Cr-O-N coatings with different oxygen concentration were synthesized by unfiltered cathodic arc evaporation in a "Bulat 3T" system (Fig. 1) on HS6-5-2 (DIN standard) steel substrates, 32 mm in diameter and 3 mm thick. was applied. A vacuum-arc plasma source equipped with Cr (99.99 %) cathode of 60 mm diameter and with magnetic stabilization of a cathode spot was used. The substrates were polished to a roughness Ra of about 0.02  $\mu\text{m}$ . Then, the substrates were chemically and ultrasonically cleaned in a hot alkaline bath for 10 min and dried in warm air. After that, they were placed on a planetary rotating holder at the distance of about 300 mm. During deposition the rotation speed was about 30 rpm.

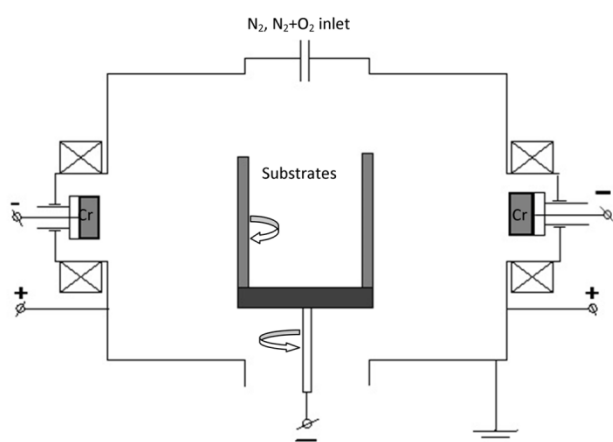


**Fig. 1.** Schematic diagram of the cathodic arc evaporation system.

Before deposition of the coatings the vacuum chamber was evacuated to a pressure of 2 mPa. The next step of substrate cleaning was ion etching by chromium ion bombardment. The etching cleaning parameters were as follows: DC bias of  $-1300\text{ V}$ , time - 3 min, the arc current - 90 A. A chromium layer (about 0.1  $\mu\text{m}$  thick) to improve the adhesion was deposited on the substrate at the bias voltage of  $-100\text{ V}$  for 5 min. Cr-O-N coatings were deposited in a  $(\text{N}_2+\text{O}_2)$  gas mixture with different relative oxygen

concentrations  $\text{O}_{2(x)}=\text{O}_2/(\text{N}_2+\text{O}_2)\%$ , where x is 0, 5, 20 and 50%. During deposition, the  $(\text{N}_2+\text{O}_2)$  gas mixture pressure and substrate temperature were kept at 1.8 Pa and about  $400^\circ\text{C}$ , respectively. The deposition was carried out for 45 min at a substrate bias voltage of  $-150\text{ V}$ . After that the coating thickness was about 7-8  $\mu\text{m}$ .

The samples were deposited in different relative oxygen concentration, 0 %, 5 %, 20 % and 50 %. The samples are denoted as Cr-O(x)-N, where x means relative oxygen concentration.

### 2.2 Coatings characterization

The topography, coefficient of friction, friction force and the wear in microscale of Cr-O-N coatings were investigated using AFM device HT-206 (produced by MTM Belarus).

Four different AFM probes were used in these investigations - two standard silicon probes (for roughness measurements and friction) and two diamond tips (on a silicon and a steel cantilever - for friction and wear measurements, respectively). The probes had different stiffness of cantilever, different tip's radius and different tip's material. Probes with different stiffness of cantilevers allow to study friction force and friction coefficient on the Cr-O-N coatings at different load. Diamond probe simulates the contact of the coating with indenter during scratch testing and with a tool during machining. The low and the high load on the surface provide possibility to study the Cr-O-N coatings in the condition of the sliding regime and the boundary regime between the sliding and the ploughing process [21].

Roughness measurements in the contact mode were made using a sharp, microfabricated silicon probe type CSC38 mounted on a rectangular cantilever beam (Micromash, Estonia). Friction coefficient and friction forces were determined using standard silicon probe with V-shape cantilever (Micromash, Estonia), and a diamond tip on the silicon cantilever (TipsNano, Estonia) signed as Diamond 1 and a diamond tip on the steel cantilever (R-DEC Co., Japan) signed as Diamond 2. The characteristics of probes are shown in the Tab. 1. The test conditions in scanning, friction and wear investigations are summarized in the Tab. 2.

**Table 1.** Characteristics of cantilevers used in Cr-O-N coatings investigations.

Test	Type of testing			
	Surface scanning	Microfriction by scanning		Microwear and friction by wear
Type of probe tip	Si	Si	Diamond 1	Diamond 2
Tip radius [nm]	10	50	10	270
Cantilever stiffness [N/m]	0.08	3.1	85	1991
Poisson ratio	0.266	0.266	0.07	0.07
Elastic modulus [GPa]	131	131	1140	1140
Microhardness [GPa]	12	12	100	100

**Table 2.** Test conditions during AFM tests.

Test	Type of testing			
	Surface scanning	Friction		Wear
Type of probe tip	Si	Si	Diamond 1	Diamond 2
Number of scans	1	1	1	4
Number of line/scan	256	256	256	256
Scan length [ $\mu\text{m}$ ]	20	20	20	5
Scan area [ $\mu\text{m}^2$ ]	20 × 20	20 × 20	20 × 20	5 × 5
Load [ $\mu\text{N}$ ]	0.005	0.14	0.230	1400
Speed [ $\mu\text{m/s}$ ]	2 - 17	17	17	4.3

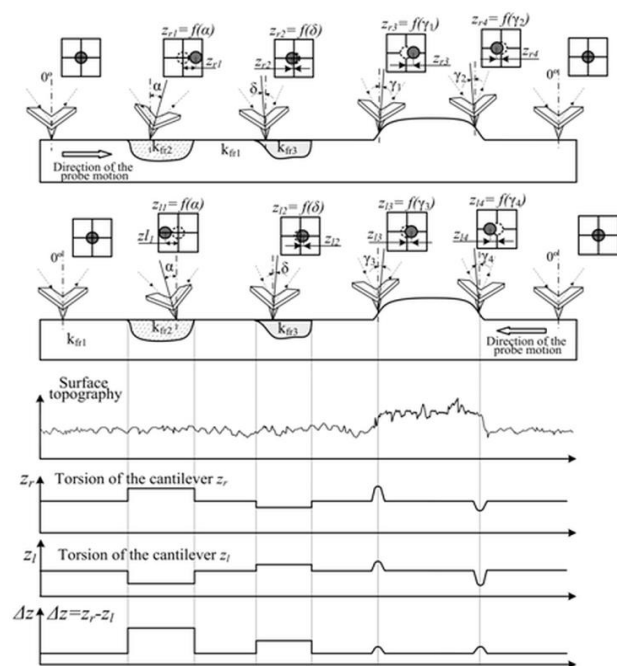


**Fig. 2.** Two fold scanning during one line for friction forces determination and cantilever twist because of friction forces acting.

To measure the friction force the AFM probe scans the surface in so-called two pass method [22], Fig. 2. During one pass the probe goes forward in a direction perpendicular to the long axis of the cantilever beam. The deflection of the cantilever which determines the load on the surface is maintained by the feedback circuitry on

the preset value. When the probe returns back in the second pass, it moves according to the first line, which suits to the relief of the surface. During the forward and the back ways the friction forces act from the surface on a tip, which cause the torsion of the cantilever besides the cantilever's deflection in the normal direction. The angle of this twist depends on the value of friction force. It can be determined from the difference between lines  $\Delta Z$  marked cantilever position during passing in forward and in back directions across Cr-O-N coating (Fig. 3).

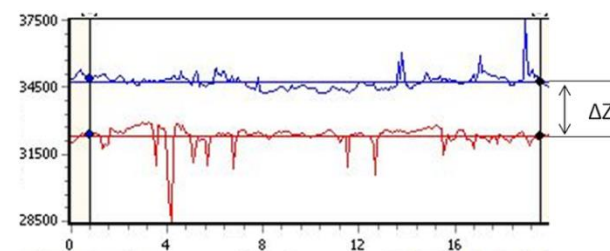


**Fig. 3.** Profiles of the lateral cantilever deflection between passing in forward and in back directions across Cr-O-N coating to determine of  $\Delta Z$ .

To avoid the misalignment between the laser beam and the photodetector axis which would introduce error in the measurement the two pass methods were developed. It allows to avoid an error caused by the developed relief of the surface. To re-calculate the signal from the twist of the

cantilever on photodetector of AFM into force value the force calibration of cantilever is used.

The coefficient of friction is calculated from a ratio of the force of friction between two bodies and the normal force pressing them together. Friction force  $F$  for the probe with V-shape cantilever was calculated according to the formula [21]:

$$F = \frac{dz \cdot l \cdot k}{3 \cdot s \cdot (1 + \nu)}. \quad (1)$$

Friction force  $F$  for the probe with rectangular cantilever was calculated according to the formula [21]:

$$F = \frac{dz \cdot r \cdot G \cdot h^3 \cdot b}{l^2 \cdot s}, \quad (2)$$

where:  $dz = \Delta z/2$  – the value of the lateral cantilever deflection between passing in forward and back directions, divided by 2 (Fig. 2),  
 $k$  – cantilever stiffness,  
 $G$  – shear modulus of cantilever material,  
 $\nu$  – Poisson's ratio,  
 $r$  – constant,  $r = 0.333$  for  $b/h > 10$ ,  
 $l, h, b$  – the length, thickness and width of cantilever,  
 $s$  – the height of the probe tip.

The force calibration procedure is very important in AFM force measurement not only for force resolution, but because of the fact that in microfriction the friction force and coefficient of friction are dependent on the load. The force calibration manual operation according to the type of probe and cantilever stiffness using penetration in silicon and diamond polished plates was carried out.

To study the wear resistance of the coating a probe as a diamond tip (three-sided pyramid shape) mounted with a steel cantilever was used. The test of wear resistance was performed with load about 1.4 mN, 4 scans on the same surface, 256 lines in scan on the scan area  $5 \times 5 \mu\text{m}^2$ . Cr-O(20)-N, the most wear resistant sample of the set was worn by 14 scans. The image of the wear track was visualized by the same diamond probe with load about 300  $\mu\text{N}$ . The wear rate was calculated according to Archard's formula [23]:

$$k_v = \frac{V}{Ls},$$

where  $V$  is the wear volume,  $s$  - sliding distance and  $L$  - applied normal load.

The friction force and coefficient of friction were calculated from the scans obtained during the wear to study the friction in a boundary regime between the sliding and ploughing process.

### 3. RESULTS AND DISCUSSION

The main feature of the microfriction test using AFM is the high contact pressure due to a small contact area. For tested system of Cr-O-N coatings it can range from several GPa to hundred of GPa in comparison to macrotest on friction with contact pressure about 1.3 GPa (Tab. 3). Relatively small normal load amounted to 1.4 mN should not generate Hertzian stresses and in consequence plastic deformation of tested coatings in macrolevel. However this normal load recalculated according to contact area of diamond tip with diameter about 540 nm can provide the significant stresses (Tab. 3). Due to the fact that sliding speed influences the coefficient of friction and wear of the coating all tests were conducted at the same velocity.

Due to application of different cantilevers their stiffness provides the different pressing forces on the coating surface from nN to mN. It creates maximal Hertzian stresses ranged from 7.5 GPa (for Si probe) to 105.9 GPa (diamond probe), Tab. 3. It allows to study both the processes of friction in the sliding regime on the real coating surface and the wear of the top layer of the coatings.

Above values were calculated using AMES website [24]. They indicate that Hertzian stress in wear using AFM is high, above 100 GPa.

In typical pin-on-disc test with  $\text{Al}_2\text{O}_3$  ball as a counterpart and normal load of 20 N it is much lower, about 1.3 GPa. It means that wear process in micro-scale (AFM) is probably more effective than in macro-scale. The values of coefficient of friction and friction force obtained using different types of probes during AFM - friction test are shown in Fig. 4.

**Table 3.** Comparison of contact stresses during AFM tests.

Parameters of testing	Type of the test			
	Microfriction by scanning		Microwear (microfriction by wear)	Macrofriction*
Type of probe tip	Si	Diamond 1	Diamond 2	Al <sub>2</sub> O <sub>3</sub> ball
Force [N]	1.4×10 <sup>-7</sup>	2.3×10 <sup>-7</sup>	1.4×10 <sup>-3</sup>	20
Max Hertzian stresses** [GPa]	7.5 - 7.7	42.8 - 52.3	98.8 - 105.9	1.26 - 1.34
Max share stresses** [GPa]	2.2 - 2.3	12.9 - 15.8	29.9 - 32.1	0.37 - 0.40
Depth of max stresses**	1- 2 nm	6 - 7 nm	40 - 50 nm	20 - 70 μm

\* according to data presented in [20]

\*\* for Cr-O-N coatings with  $H = 19 - 30$  GPa,  $E = 292 - 335$  GPa [20]

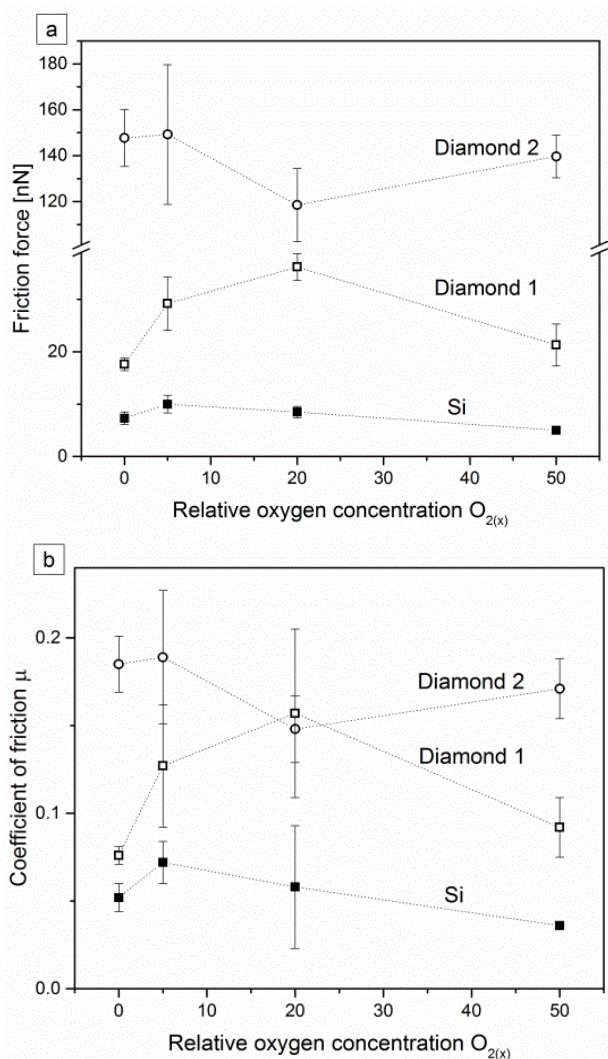
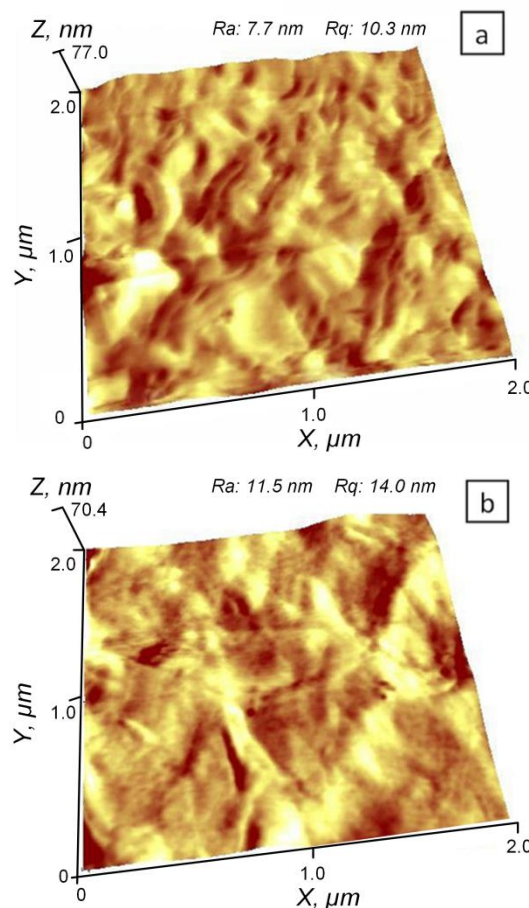


**Fig. 4.** Friction force (a) and coefficient of friction (b) for Cr-O-N coatings tested in sliding (Si probe, diamond 1) and ploughing (diamond 2) regimes.

For silicon probe the coefficient of friction of coatings investigated ranges from 0.036 to 0.072. The friction forces in above tests were from 5 to 10 nN (Fig. 4). Such small values of the friction forces can be explained by the low normal load and by the small size of the contact area. The values of friction forces obtained by

silicon probe correlate to the surface roughness. According to the value of normal load for this probe it is the classical sliding regime [25,26].

The Ra roughness, calculated for the area 2 × 2 μm<sup>2</sup>, ranged from 7.3 to 11.5 nm. In microfriction the real contact area of the tip should be considered. The surface of CrN and Cr-O-N coatings contains grains and subgrains (Figs. 5a - 5d). The diameter of grains is 200 - 400 nm for Cr-(0)-N, 400 - 600 nm for Cr-(5)-N, 200 - 300 nm Cr-O(20)-N and Cr-O(50)-N coatings. The diameter of subgrains is 50 - 100 nm for all coatings, Fig. 6 [9].



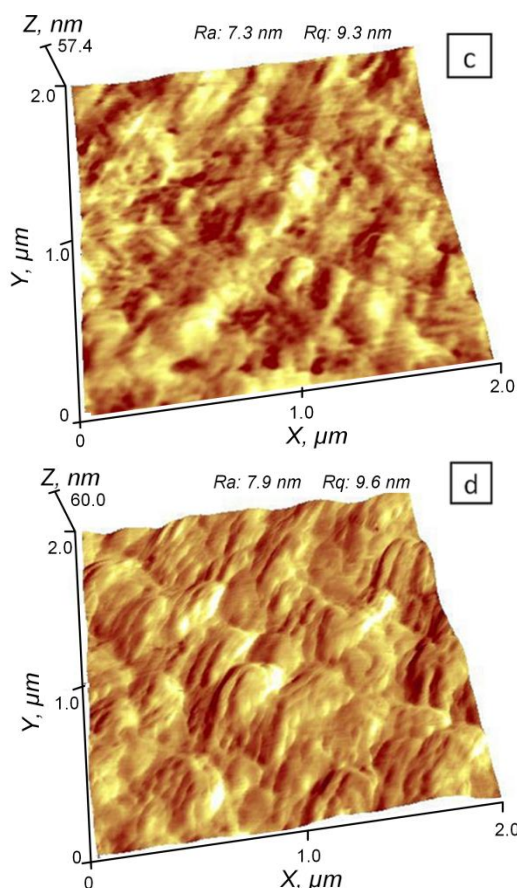


**Fig. 5.** AFM images of CrON coating surface, scanning area  $2 \times 2 \mu\text{m}^2$ : a) CrN, b) Cr-O(5)-N, c) Cr-O(20)-N, d) Cr-O(50)-N.

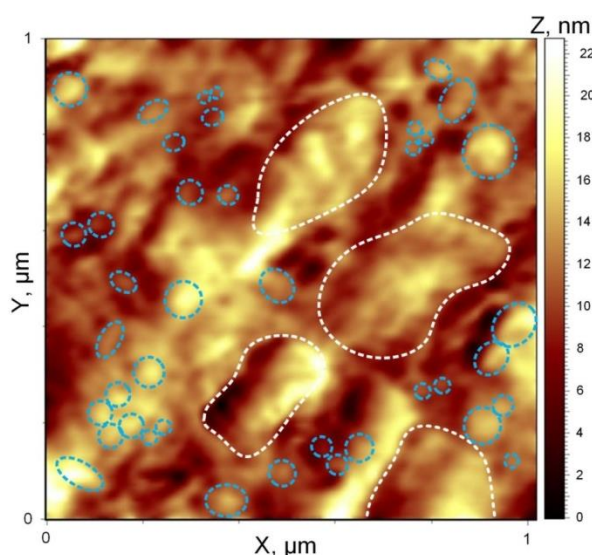


**Fig. 6.** AFM-microstructure of Cr-O(20)-N coating with big grains and small subgrains, scanning area  $1.0 \times 1.0 \mu\text{m}^2$ . White dotted lines suggest the boundaries of big grains and blue dotted lines point at subgrain boundaries.

The size of grains is proportional to the tip size of the diamond probe for wear and the size of subgrains which is proportional to the tip size of

silicon probe and to the size of the diamond probe for friction.

The diamond 1 probe for friction has a smaller radius (10 nm) than a silicon probe (50 nm). The friction forces and friction coefficients obtained using diamond probe are higher and ranges from 17 to 36 nN and from 0.076 to 0.157, respectively. This fact is explained by the higher normal load (230 nN) and the other chemical nature of the diamond. As it was found earlier, increase in the normal load on the diamond AFM probe in the sliding regime leads to the increase of friction force [27].

Both probes (silicon and diamond 1) with the load 140 – 230 nN provide the sliding regime on the Cr-O-N coatings surface. In this cause the dynamic of friction forces and friction coefficients with oxygen concentration in Cr-O-N coatings are similar to silicon and diamond probes.

The dynamic of friction forces and friction coefficients with oxygen concentration in Cr-O-N coatings for diamond 2 probe for wear differs from two first probes. Because of the high normal load about  $1400 \mu\text{N}$  the contact between the probe and surface is not sliding but ploughing. As it was found earlier [28] the AFM diamond probe during the scratch of the material surface by machining begin the process with full elastic recovery, then follows ploughing and then nano-cutting. The first stage is completely elastic and the other two are partly elastic. The ploughing by AFM probe in the mesoscopic scale can be special and do not destroy material by cracking. The friction forces and friction coefficients obtained with diamond 2 probe range from  $118 \mu\text{N}$  to  $149 \mu\text{N}$  and from 0.148 to 0.185, respectively. The other regime of interaction between the probe and the surface changed the dynamic of dependence of friction forces and coefficients of friction from oxygen concentration in Cr-O-N coatings. The lowest values in this case has Cr-O(20)-N coating.

The coefficient of friction for mentioned coatings in macroscale (normal load 20 N) presented in [20] ranged from 0.48 to 0.65. It is in the agreement with the results of work [29], where the friction force increase with the normal load.

The results of the coefficient of friction and friction force determined for Cr-O-N coatings using the diamond probe at load of  $1400 \mu\text{N}$  in

the plouding regime dependent on the number of scans during wear test are shown in Fig. 7.

Standard deviation for coefficient of friction using diamond probe and load 1400  $\mu\text{N}$  ranged from 9 to 20 % and for silicon probe (load 140 nN) it ranged from 6 to 60 %. It means that the friction conditions at load of 1400  $\mu\text{N}$  are more stable. The lowest coefficient of friction was determined for Cr-O(20)-N coating. Alternate increase and decrease of coefficient of friction value from point to point during the coatings wear can be explained by moving of worn material in one scan and smoothing during the next one (Fig. 7c). Therefore the coefficient of friction in deeper layers from the surface can differ from the one on the surface due to surface smoothing and involving in friction process the other phases into Cr-O-N coatings. These results are in the agreement with previous findings [30] where the friction force decrease from scan to scan because of scanning-induced reduction of adhesion energy of the surface.

Because the friction tests were carried out on air with humidity of about 20 % the thin water film condensed from air was probably between the tip and the coating [21]. The water film in the

real contact promotes the increase of adhesion forces between the tip and the coating and causes the decrease of friction force and coefficient of friction [37]. In macro-scale, as in ball-on-disc test, the thin water film between rubbing materials reduces coefficient of friction below 100 °C [38].

The wear depth after the test for coatings with increasing oxygen amount was 80 nm, 30 nm, 10 nm, 100 nm per 4 scans, respectively, Fig. 8. The most resistant to wear was Cr-O(20)-N coating. Due to small wear depth the test was repeated with higher number of scans. After 14 scans the wear track depth was 40 nm. The lowest wear rate shows Cr-Cr-O(20)-N coating -  $2.0 \times 10^{-14}$   $\text{m}^3/\text{Nm}$ , and the highest -  $2.0 \times 10^{-13}$   $\text{m}^3/\text{Nm}$  shows Cr-O(50)-N coating. Calculated values of wear rate are gathered in Tab. 4.

Above results for CrN are generally at least one level higher than obtained in tests with higher load. Essen et al. [13] found in pin-on-disc test the specific wear rate ranged from  $7 \times 10^{-16}$  to  $2 \times 10^{-15}$   $\text{m}^3/\text{Nm}$  dependent on the test parameters and coating composition.

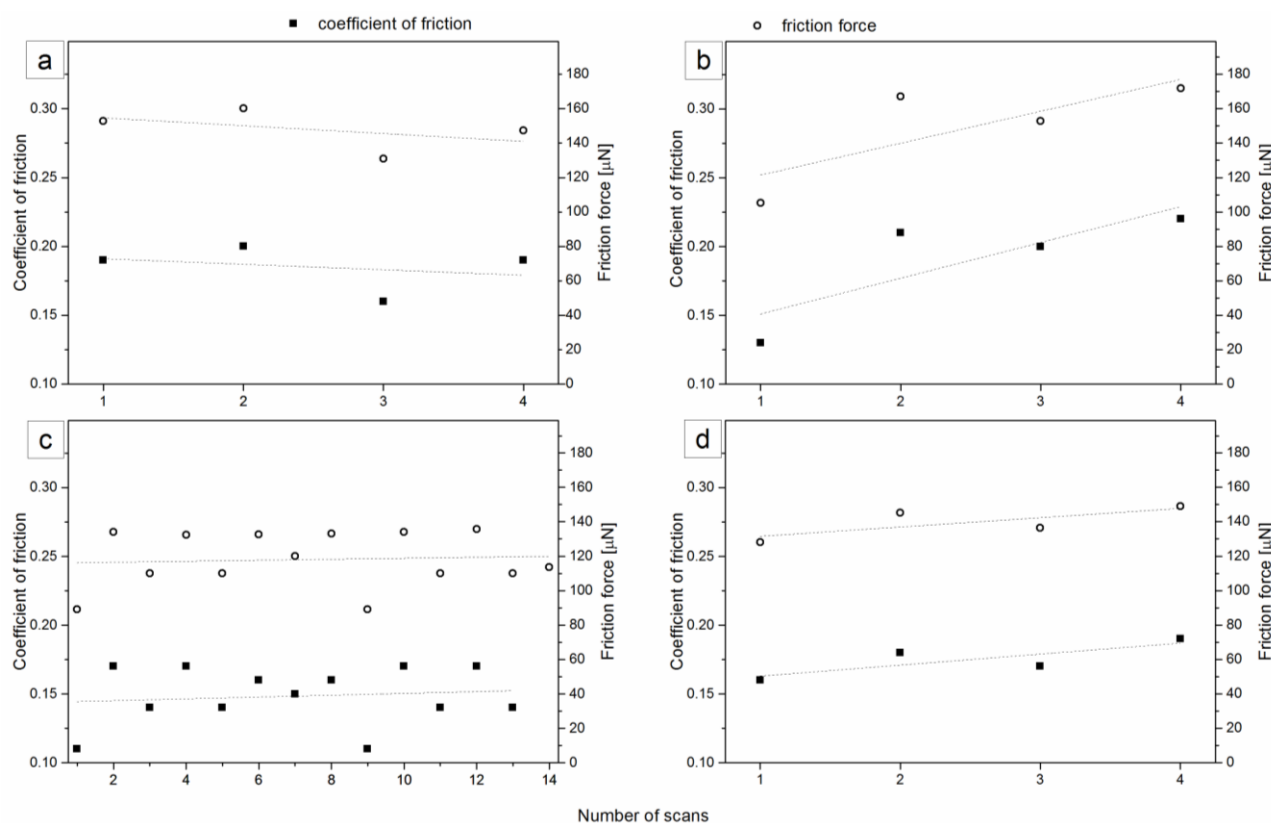


**Fig. 7.** Friction force and coefficient of friction for CrON coatings during the wear by diamond tip: a) CrN, b) Cr-O(5)-N, c) Cr-O(20)-N, d) Cr-O(50)-N.

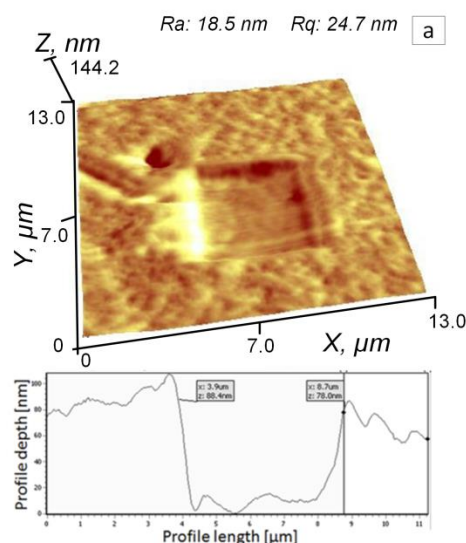
**Table 4.** Results of the roughness, friction test and wear of Cr-O-N coatings tested by AFM.

Type of testing	Tip	Characteristic	Coating			
			Cr-O(0)-N	Cr-O(5)-N	Cr-O(20)-N	Cr-O(50)-N
Surface scanning	Silicon	Roughness on area 2 × 2 μm <sup>2</sup> [nm]	7.7	11.5	7.3	7.9
Wear	Diamond	Depth of wear [nm]	80	30	40	100
		Depth of wear/one scan [nm]	20	7.5	2.9	25
		Wear rate [m <sup>3</sup> /Nm]	1.6×10 <sup>-13</sup>	6.1×10 <sup>-14</sup>	2.0×10 <sup>-14</sup>	2.0×10 <sup>-13</sup>

Ehiasarian et al. [12] found similar results in the range of  $2.3 \times 10^{-16} \div 1.5 \times 10^{-14}$  m<sup>3</sup>/Nm dependent on deposition method. It is known that CrN coatings can be deposited using magnetron sputtering, arc evaporation or HIPIMS. CrN coatings deposited by HIPIMS show a dense coating with strong bonding between the columns. This microstructure can probably respond for very low wear rate -  $2.3 \times 10^{-16}$  m<sup>3</sup>/Nm. To assess the wear resistance the abrasive wear tests based on the ball-cratering method was conducted. Drnovšek et al. using the tribometer set to reciprocal sliding mode equipped with Al<sub>2</sub>O<sub>3</sub> ball as a counterbody found wear rate of  $1.2 \times 10^{-15}$  m<sup>3</sup>/Nm [14].

These higher wear rate values found in AFM wear test ( $2.0 \times 10^{-13} \div 2.0 \times 10^{-14}$  m<sup>3</sup>/Nm) are probably connected with high stresses generated in tip-coating contact. But the second reason of overestimated wear values obtained using AFM in comparison with classical pin-on-disk test realized often by CSM tribometer is using the Al<sub>2</sub>O<sub>3</sub> ball. In work [15] Al<sub>2</sub>O<sub>3</sub> ball with significantly lower hardness compared to coatings tested was used as a counterbody. The Al<sub>2</sub>O<sub>3</sub> ball is widely used in wear testing of hard coatings and the results can be better compared to those in the literature. But the depth of wear track in the coating in this case includes only a part of system wear. The second part includes counterbody wear. In addition, it is necessary to take into account the speed of movement of the counterbody during worn surface - than the higher it is, the less the wear is [21]. The speed of the counterbody moving in all macrodevices is several times higher than in the AFM.

In the wear tracks on the surface of Cr-O-N coatings only abrasion of the thin surface layer of nanometric size was observed. Due to the fact that no other effect (i.e. cracking) was found the coefficient of friction was lower. In microfriction processes at the high contact stresses, the maximum shear stresses in the material are localized at the depth of several nanometers (Tab. 3). Due to the high contact stresses in the very thin layer with a thickness of nanometers the plastic deformation can be present there. The thin sublayer of the plastically deformed material loses its mechanical properties and therefore is easy to remove from the surface. In this case, it is not possible to distinguish abrasive friction from ploughing. Microfriction has its own mechanism - shear for nanometer layers of material. In such conditions, ploughing or abrasive friction in its clear form are not observed. Thus, microdevices experience the special conditions in the contact with the boundary regime of sliding and ploughing.



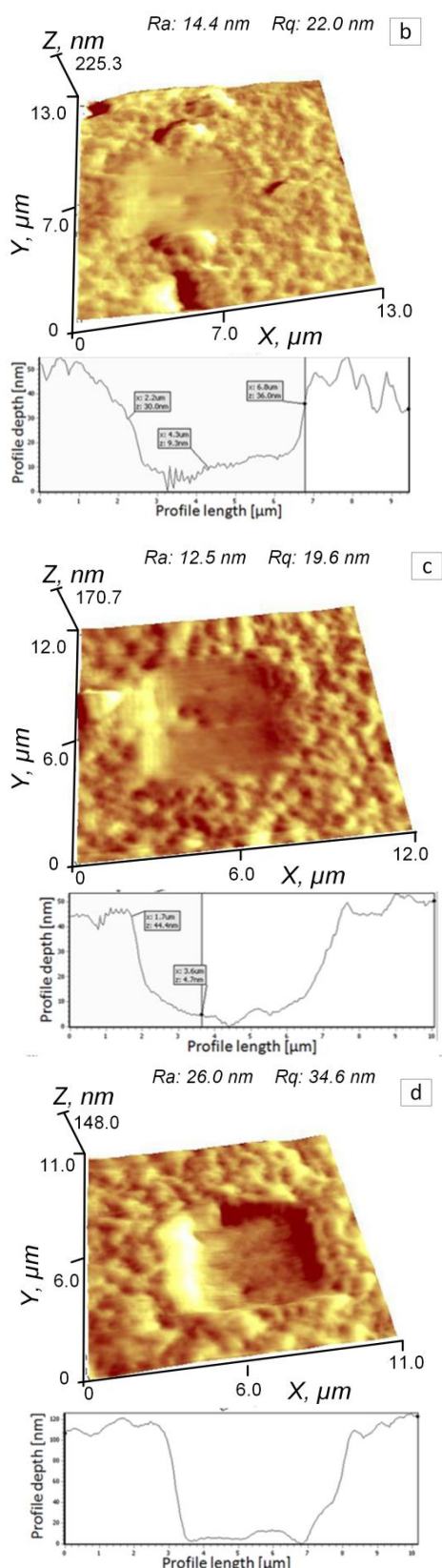


**Fig. 8.** Result of the wear of Cr-O-N coatings: (a) Cr-O(0)-N, (b) Cr-O(5)-N, (c) Cr-O(20)-N, (d) Cr-O(50)-N.

The best tribological properties among Cr-O-N coatings were found for Cr-O(20)-N because of its smallest grain [9] and highest microhardness [31].

This created the conditions for the easier shift of the near -surface nanometer layers under the high contact load at a sufficiently high level of microhardness.

#### 4. CONCLUSIONS

The tribological properties (friction and wear) of Cr-O-N coatings were tested in microscale by atomic force microscopy. An application of different probes (Si and diamond) allows to determine their interaction with the tested coatings. Analysis of the results of the roughness, friction and wear suggests as follows:

- the low coefficient of friction (0.036) and friction force (5.0 nN) in sliding regime are not correlated with the low wear rate of Cr-O(50)-N coating, consisted from Cr<sub>2</sub>O<sub>3</sub> phase. It is one of the highest and is  $2.0 \times 10^{-13} \text{ m}^3/\text{Nm}$ . The low coefficient of friction (0.148) and friction force (118.48  $\mu\text{N}$ ) in ploughing regime (abrasion by thin nanometric layers) are good correlated with the low wear rate of Cr-O(20)-N coating, consisted from CrN phase. It is the lowest and is  $2.0 \times 10^{-14} \text{ m}^3/\text{Nm}$ .
- Hertzian stresses were calculated for every type of the contact. It was found that in wear tests the Hertzian stresses are about 90-100 GPa for investigated coatings, much higher than in macro-wear. It is probably connected with small contact area connected with the radius of probe tip used.
- microdevices experience the special conditions in the contact - shear for nanometer layers of material.

The correlation between coating properties in macro-scale and micro (nano)-scale is a great research challenge due to different mechanism of acting, and the interpretation of results should be later conducted.

#### REFERENCES

[1] L. Castaldi, D. Kurapov, A. Reiter, V. Shklover, P. Schwaller, J. Patscheider, *Effect of the oxygen content on the structure, morphology and oxidation resistance of Cr-O-N coatings*, Surface and Coatings Technology, vol. 203, iss. 5-7, pp. 545-549, 2008, doi: 10.1016/j.surfcoat.2008.05.018

- [2] T. Wierzchoń, I. Ulbin-Pokorska, K. Sikorski, *Corrosion resistance of chromium nitride and oxynitride layers produced under glow discharge conditions*, Surface and Coatings Technology, vol. 130, iss. 2-3, pp. 274-279, 2000, doi: [10.1016/S0257-8972\(00\)00696-4](https://doi.org/10.1016/S0257-8972(00)00696-4)
- [3] S. Agouram, F. Bodart, G. Terwagne, *Characterisation of reactive unbalanced magnetron sputtered chromium oxynitride thin films with air*, Surface and Coatings Technology, vol. 180-181, pp. 164-168, 2004, doi: [10.1016/j.surfcoat.2003.10.060](https://doi.org/10.1016/j.surfcoat.2003.10.060)
- [4] T. Suzuki, J. Inoue, H. Saito, M. Hirai, H. Suematsu, W. Jiang, K. Yatsui, *Influence of oxygen content on structure and hardness of Cr-N-O thin films prepared by pulsed laser deposition*, Thin Solid Films, vol. 515, iss. 4, pp. 2161-2166, 2006, doi: [10.1016/j.tsf.2006.05.007](https://doi.org/10.1016/j.tsf.2006.05.007)
- [5] S. Collard, H. Kupfer, G. Hecht, W. Hoyer, H. Moussaoui, *The reactive magnetron deposition of CrN<sub>x</sub>O<sub>y</sub> films: first results of property investigations*, Surface and Coatings Technology, vol. 112, iss. 1-3, pp. 181-184, 1999, doi: [10.1016/S0257-8972\(98\)00752-X](https://doi.org/10.1016/S0257-8972(98)00752-X)
- [6] J.S. Yun, Y.S. Hong, K.H. Kim, *Characteristics of Ternary Cr-O-N Coatings Synthesized by Using an Arc Ion Plating Technique*, Journal of the Korean Physical Society, vol. 57, no. 1, pp. 103-110, 2010, doi: [10.3938/jkps.57.10](https://doi.org/10.3938/jkps.57.10)
- [7] M. Urgen V. Ezirmik, E. Senel, Z. Kahraman, K. Kazmanli, *The effect of oxygen content on the temperature dependent tribological behavior of Cr-O-N coatings*, Surface & Coatings Technology, vol. 203, iss. 16, pp. 2272-2277, 2009, doi: [10.1016/j.surfcoat.2009.02.027](https://doi.org/10.1016/j.surfcoat.2009.02.027)
- [8] A.S. Kuprin, T.A. Kuznetsova, A. Gilewicz, G.N. Tolmachova, V.D. Ovcharenko, S. O. Abetkovskaia, T.I. Zubar, A.L. Khudoley, S.A. Chizhik, O. Lupicka, B. Warcholinski, *Tribological properties of vacuum arc Cr-O-N coatings in macro- and microscale*, Problems of Atomic Science and Technology, vol. 6, no. 106, pp. 211-214, 2016.
- [9] B. Warcholinski, A. Gilewicz, O. Lupicka, A.S. Kuprin, G.N. Tolmachova, V.D. Ovcharenko, I.V. Kolodiy, M. Sawczak, A.E. Kochmanska, P. Kochmanski, T.A. Kuznetsova, T.I. Zubar, A.L. Khudoley, S.A. Chizhik, *Structure of CrON coatings formed in vacuum arc plasma fluxes*, Surface and Coatings Technology, vol. 309, pp. 920-930, 2017, doi: [10.1016/j.surfcoat.2016.10.061](https://doi.org/10.1016/j.surfcoat.2016.10.061)
- [10] T. Minami, S. Nishio, Y. Murata, *Periodic microstructures of Cr-O-N coatings deposited by arc ion plating*, Surface and Coatings Technology, vol. 254, pp. 402-409, 2014, doi: [10.1016/j.surfcoat.2014.06.051](https://doi.org/10.1016/j.surfcoat.2014.06.051)
- [11] R. Cecchini, A. Fabrizi, M. Cabibbo, C. Paternoster, B.N. Mavrin, V.N. Denisov, N.N. Novikova, M. Haïdopoulo, *Mechanical, microstructural and oxidation properties of reactively sputtered thin Cr-N coatings on steel*, Thin Solid Films, vol. 519, iss. 19, pp. 6515-6521, 2011, doi: [10.1016/j.tsf.2011.04.115](https://doi.org/10.1016/j.tsf.2011.04.115)
- [12] A.P. Ehiasarian, P.E. Hovsepian, L. Hultman, U. Helmersson, *Comparison of microstructure and mechanical properties of chromium nitride-based coatings deposited by high power impulse magnetron sputtering and by the combined steered cathodic arc/unbalanced magnetron technique*, Thin Solid Films, vol. 457, iss. 2, pp. 270-277, 2004, doi: [10.1016/j.tsf.2003.11.113](https://doi.org/10.1016/j.tsf.2003.11.113)
- [13] P. van Essen, R. Hoy, J.D. Kamminga, A.P. Ehiasarian, G.C.A.M. Janssen, *Scratch resistance and wear of CrN<sub>x</sub> coatings*, Surface and Coatings Technology, vol. 200, iss. 11, pp. 3496-3502, 2006, doi: [10.1016/j.surfcoat.2004.09.020](https://doi.org/10.1016/j.surfcoat.2004.09.020)
- [14] A. Drnovšek, P. Panjan, M. Panjan, S. Paskvale, J. Buh, M. Čekada, *The influence of surrounding atmosphere on tribological properties of hard protective coatings*, Surface and Coatings Technology, vol. 267, pp. 15-20, 2015, doi: [10.1016/j.surfcoat.2014.11.068](https://doi.org/10.1016/j.surfcoat.2014.11.068)
- [15] B. Warcholinski, A. Gilewicz, *Mechanical properties of multilayer TiAlN/CrN coatings deposited by cathodic arc evaporation*, Surface Engineering, vol. 27, iss. 7, pp. 491-497, 2011, doi: [10.1179/026708410X12786785573355](https://doi.org/10.1179/026708410X12786785573355)
- [16] P.Z. Shi, J. Wang, C.X. Tian, Z.G. Li, G.D. Zhang, D.J. Fu, B. Yang, *Structure, mechanical and tribological properties of CrN thick coatings deposited by circular combined tubular arc ion plating*, Surface and Coatings Technology, vol. 228, sup. 1, pp. S534-S537, 2013, doi: [10.1016/j.surfcoat.2012.04.041](https://doi.org/10.1016/j.surfcoat.2012.04.041)
- [17] S.A. Chizhik, Z. Rymuza, V.V. Chikunov, T.A. Kuznetsova, D. Jarzabek, *Micro- and nanoscale testing of tribomechanical properties of surfaces*, in R. Jablonski (Ed.) et al.: Recent advances in mechatronics, Springer, Leipzig, pp. 541-545, 2007.
- [18] V. Anishchik, V. Uglov, A. Kuleshov, A. Filipp, D. Rusalsky, M. Astashynskaya, M. Samtsov, T. Kuznetsova, F. Thiery, Y. Pauleau, *Electron field emission and surface morphology of a-C and a-C:H thin films*, Thin Solid Films, vol. 482, iss. 1-2, pp. 248-252, 2005, doi: [10.1016/j.tsf.2004.11.153](https://doi.org/10.1016/j.tsf.2004.11.153)
- [19] P.A. Vityaz, A.I. Komarov, V.I. Komarova, T.A. Kuznetsova, *Peculiarities of triboformation of wear-resistant layers on the surface of a MAO-coating modified by fullerenes*, Journal of Friction and Wear, vol. 32, no. 4, pp. 313-325, 2011, doi: [10.3103/S106836661104012X](https://doi.org/10.3103/S106836661104012X)

- [20] B. Warcholinski, A. Gilewicz, A.S. Kuprin, G.N. Tolmachova, V.D. Ovcharenko, T.A. Kuznetsova, T.I. Zubar, A.L. Khudoley, S.A. Chizhik, *Mechanical properties of Cr-O-N coatings deposited by cathodic arc evaporation*, Vacuum, vol. 156, pp. 97-107, 2018, doi: [10.1016/j.vacuum.2018.07.017](https://doi.org/10.1016/j.vacuum.2018.07.017)
- [21] B. Bhushan, *Nanotribology and nanomechanics, An Introduction*, 2<sup>nd</sup> ed., Berlin Heidelberg: Springer-Verlag, 2008.
- [22] T.A. Kuznetsova, T.I. Zubar, V.A. Lapitskaya, K.A. Sudzilouskaya, S.A. Chizhik, A.L. Didenko, V.M. Svetlichnyi, M.E. Vylegzhanina, T.E. Sukhanova, *Tribology properties investigation of the thermoplastic elastomers surface with the AFM lateral forces mode*, IOP Conference Series: Materials Science and Engineering, vol. 256, 012022, 2017, doi: [10.1088/1757-899X/256/1/012022](https://doi.org/10.1088/1757-899X/256/1/012022)
- [23] J.F. Archard, *Contact and rubbing of flat surface*, Journal of Applied Physics, vol. 24, iss. 8, pp. 981-988, 1953, doi: [10.1063/1.1721448](https://doi.org/10.1063/1.1721448)
- [24] Hertzian contact, available at: <http://www.amesweb.info/HertzianContact/HertzianContact.aspx>, accessed: 18.02.2019.
- [25] J.L. Bosse, S. Lee, A.S. Andersen, D.S. Sutherland, B.D. Huey, *High Speed Friction Microscopy and Nanoscale Friction Coefficient Mapping*, Measurement Science and Technology, vol. 25, no. 11, 2014, doi: [10.1088/0957-0233/25/11/115401](https://doi.org/10.1088/0957-0233/25/11/115401)
- [26] U. Celano, Feng-Chun Hsia, D. Vanhaeren, K. Paredis, Torbjörn E. M. Nordling, Josephus G. Buijnsters, T. Hantschel, W. Vandervorst, *Mesoscopic physical removal of material using sliding nano-diamond contacts*, Scientific Reports, vol. 8, no. 2994, 2018, doi: [10.1038/s41598-018-21171-w](https://doi.org/10.1038/s41598-018-21171-w)
- [27] N.T. Garabedian, H.S. Khare, R.W. Carpick, D.L. Burris, *AFM at the Macroscale: Methods to Fabricate and Calibrate Probes for Millinewton Force Measurements*, Tribology Letters, vol. 67, iss. 21, 2019, doi: [10.1007/s11249-019-1134-2](https://doi.org/10.1007/s11249-019-1134-2)
- [28] A. Elkaseer, E.B. Brousseau, *Modelling the surface generation process during AFM probe-based machining: simulation and experimental validation*, Surface Topography: Metrology and Properties, vol. 2, no. 2, 2014, doi: [10.1088/2051-672X/2/2/025001](https://doi.org/10.1088/2051-672X/2/2/025001)
- [29] G. Gao, R.J. Cannara, R.W. Carpick, J.A. Harrison, *Atomic-Scale Friction on Diamond: A Comparison of Different Sliding Directions on (001) and (111) Surfaces Using MD and AFM*, Langmuir, vol. 23, no. 10, pp. 5394-5405, 2007, doi: [10.1021/la062254p](https://doi.org/10.1021/la062254p)
- [30] R.W. Carpick, M. Salmeron, *Scratching the Surface: Fundamental Investigations of Tribology with Atomic Force Microscopy*, Chemical Reviews, vol. 97, no. 4, pp. 1163-1194, 1997, doi: [10.1021/cr960068q](https://doi.org/10.1021/cr960068q)
- [31] W. Gulbinski, D. Pailharey, T. Suszko, Y. Mathey, *Study of the influence of adsorbed water on AFM friction measurements on molybdenum trioxide thin films*, Surface Science, vol. 475, iss. 1-3, pp. 149-158, 2001, doi: [10.1016/S0039-6028\(00\)01101-8](https://doi.org/10.1016/S0039-6028(00)01101-8)
- [32] T.A. Kuznetsova, T.I. Zubar, V.A. Lapitskaya, K.A. Sudilovskaya, S.A. Chizhik, V.V. Uglov, V.I. Shimanskii, N.T. Kvasov, *Atomic-Force Microscopy in the Study of the Tribological Characteristics of Thin Al-Si-N Coatings*, Journal of Surface Investigation. X-Ray, Synchrotron and Neutron Techniques, vol. 13, iss. 1, pp. 36-40, 2019, doi: [10.1134/S1027451019010117](https://doi.org/10.1134/S1027451019010117)